JSR Publications

Available Online

J. Sci. Res. **17** (3), 861-868 (2025)

JOURNAL OF SCIENTIFIC RESEARCH

www.banglajol.info/index.php/JSR

Design and Analysis of Antireflection Coatings for Silicon Solar Cells using Copper-Nanoparticles

R. Sharma*, A. Virdi

Model Institute of Engineering and Technology, Kot Bhalwal, Jammu, Jammu & Kashmir – 181122, India

Received 27 January 2025, accepted in final revised form 16 June 2025

Abstract

Silicon solar cells, despite their widespread use due to their efficiency, cost-effectiveness, and reliability, suffer from low absorption and high reflectance, limiting their performance. In this work an attempt has been made to design a double layer antireflection coating composed of copper-nanoparticles (Cu-NPs) over silicon nitride to study the performance of silicon solar cells. Numerical calculations have been performed using transfer matrix method (TMM) to obtain the reflectance at various values of Cu-NPs radius, gap interval, and volume fraction. The refractive index of the metal nanoparticles used is wavelength dependent. Inclusion of Cu-NPs in the antireflection coating has reduced the reflectance considerably. Calculated reflectance has been used in the PC1D simulator to study performance of silicon solar cell. Results obtained for Cu-NPs based ARC were further compared with a reference cell (without ARC) and a cell with SLARC.

Keywords: Antireflection coating; Nanoparticles; Reflection; Photovoltaic efficiency; PC1D; Simulation.

doi: https://dx.doi.org/10.3329/jsr.v17i3.79427 J. Sci. Res. **17** (3), 861-868 (2025)

1. Introduction

Solar cell is a promising approach for terrestrial and space photovoltaic devices and Silicon is the most widely used material for solar cells due to its well-developed technology, exceptional balance of efficiency, cost-effectiveness, and remarkable reliability [1]. One major drawback of Silicon is its indirect energy bandgap, which reduce its absorption efficiency-especially in the visible and infrared region of the spectra, thereby limiting its overall performance [2]. Additionally, optical reflection poses another significant challenge, with over 30 % of incident light reflecting off the silicon surface, leading to considerable energy losses [3-5]. To mitigate this, the use of antireflection coatings (ARCs) on the front surface of silicon solar cells is a well-established method to reduce reflection and improve overall device efficiency [6,7]. Numerous researchers have explored single- and double- layer ARCs both theoretically and experimentally. For instance, Sharma *et al*.

* *Corresponding author*: rajinder.ash@mietjammu.in

[6] examined the effects of single and double-layer ARCs composed of various materials, while Hashmi *et al*. [8] investigated the impact of diverse ARCs using PC1D simulations. Additionally, Lien *et al*. [9], Bahrami *et al*. [10], Medhat *et al*. [11], and Sharma [12] delved into materials like SiO_2/TiO_2, Al_2O_3/TiO_2, MgF_2/Ti_2O_3, and SiNx/SiNx, respectively.

In the recent past, significant progress has been made in employing conductive nanoparticles to fabricate solar cell structures, owing to their exceptional light-trapping effectiveness within the proposed designs. Researchers have demonstrated that well placed and sized nanoparticles can effectively scatter solar radiation, substantially enhancing the performance of thin-film cells [13,14]. Numerous studies have explored the enhancement of thin-film solar cells through scattering by gold, copper and silver nanoparticles [15-18]. Atwater *et al*. [19] incorporated metal nanoparticles within the solar cell to harness the strong local field enhancement, thereby increasing absorption within the surrounding semiconductor material. According to Atwater, this localized fields can generate charge carriers in semiconductors, especially useful for materials with short diffusion lengths. Incident light can also convert into surface plasmon polaritons at the metal–semiconductor interface, guiding light laterally. This enhances absorption, particularly of long-wavelength photons, due to the solar cell's large width-to-thickness ratio. Ubeid *et al*. [20] numerically studied an antireflection coating structure containing metal nanoparticles over silicon nitride. Abuibaid *et al*. [21] have studied the triple layer ARC containing multi-type of nanoparticles cell. Mirnaziry *et al*. [25] proposed that multi-layer silicon nano-particles of submicron dimensions can be deployed as an absorber of ultra-thin solar cell.

In this paper, an attempt has been made to investigate the impact of an antireflection coating composed of metal nano-particles (copper) and silicon nitride on the performance of silicon solar cells. The optical properties of the coating are analyzed using the Transfer Matrix Method (TMM) to calculate the reflection coefficient across a range of wavelengths. The resulting reflectance data is then incorporated into PC1D simulation software to evaluate the corresponding improvement in solar cell efficiency under standard test conditions.

2. Structure of ARC

Fig. 1 shows device structure considered for investigation comprises four regions. Region 1 is a vacuum, region 2 is filled with copper nanoparticles (Cu-NPs), region 3 is a layer of silicon nitride and region 4th is of silicon. Silicon nitride is chosen as material for region 3 because of its varying refractive index and good surface passivation quality. The reflection coefficient for antireflection coating (ARC) is derived numerically by employing the transfer matrix method as it relates incident and reflected waves at the input layer with the incident and reflected waves at the output layer. According to the boundary conditions, the tangential components of the electric and magnetic fields are continuous across the interface. For single layer system, field components at first boundary are related to those at second boundary by the following expressions [22,23]:

$$E_a = E_b \cos(\delta) + B_b \left(\frac{i \sin(\delta)}{\eta}\right) \quad (1)$$

$$B_a = E_b(i\eta \sin(\delta)) + B_b \cos(\delta) \quad (2)$$

These two equations in matrix form can be expressed as:

$$\begin{bmatrix} E_a/E_b \\ B_a/E_b \end{bmatrix} = \begin{bmatrix} B \\ C \end{bmatrix} = \begin{bmatrix} cos(\delta) & \frac{i\, sin(\delta)}{\eta} \\ i\eta\, sin(\delta) & cos(\delta) \end{bmatrix} \begin{bmatrix} 1 \\ \eta_s \end{bmatrix} \quad (3)$$

where $\delta = \frac{2\pi n_1 d_1 Cos\theta_1}{\lambda_o}$ is phase thickness of film, $d_1 = \frac{\lambda_o}{4n_1}$ is the thickness of film, θ_1 is the diffraction angle related to the incidence angle θ_0 by Snell's law: $n_o\, sin\theta_o = n_1\, sin\theta_1$ and η_s is the optical admittance. Further, at normal incidence transfer matrix for double layer antireflection coating (DLARC) is [12,22,23]:

$$\begin{bmatrix} B \\ C \end{bmatrix} = \begin{bmatrix} \cos(\delta_1) & \frac{i \sin(\delta_1)}{\eta_1} \\ \eta_1 i \sin(\delta_1) & \cos(\delta_1) \end{bmatrix} \begin{bmatrix} \cos(\delta_2) & \frac{i \sin(\delta_2)}{\eta_2} \\ \eta_2 i \sin(\delta_2) & \cos(\delta_2) \end{bmatrix} \begin{bmatrix} 1 \\ \eta_s \end{bmatrix} \quad (4)$$

Thus, reflectance for a given assembly can be expressed as [23].

$$R = \left| \frac{1 - \frac{Y}{n_0}}{1 + \frac{Y}{n_0}} \right|^2 \quad (5)$$

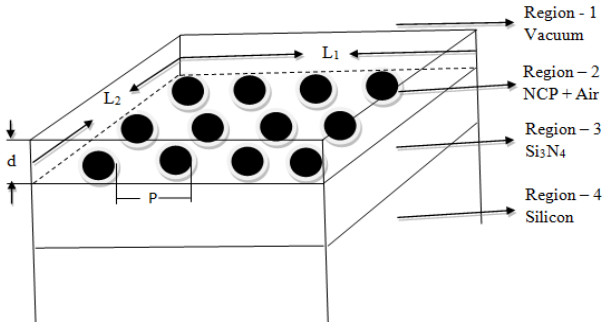

Fig. 1. Antireflection coating structure containing metal nanoparticles and silicon nitride on silicon substrate.

where Y = C/B. The effective permittivity and refractive index of the 2nd region film formed by the Cu-NPs in air are obtained by using Maxwell-Garentt medium approximation [20]:

$$\varepsilon_{eff}(\lambda) = \varepsilon_a \frac{\varepsilon_c(1+2f)+2\varepsilon_a(1-f)}{\varepsilon_c(1-f)+\varepsilon_a(2+f)} \quad (6)$$

$$n(\lambda) = \sqrt{\varepsilon_{eff}(\lambda)} \quad (7)$$

where ε_a is the permittivity of base material (air), ε_c is the permittivity of the copper nanoparticles and $f = (N_p \times V_p)/V_{layer}$ is the volume fraction of nanoparticles in the base medium (air). $N_p = (L_1/P) \times (L_2/P)$ is the number of particles on the surface, $V_{layer} = L_1 \times L_2 \times d$ is the volume of the layer of thickness d (we consider $L_1 = L_2 = 10$ cm) and $V_p = 4\pi r^3/3$ is the volume of spherical particle of radius r. Further, the permittivity of the copper (nanoparticles) can be calculated using Drude model as [20]:

$$\varepsilon_c(\lambda) = 1 - \frac{\lambda^2 \lambda_c^2}{\lambda_p^2(\lambda_c - i\lambda)} \quad (8)$$

where λ is the wavelength of the incident radiation, $\lambda_c = 4.0852 \times 10^{-5}$ m and $\lambda_p = 1.3617 \times 10^{-7}$ m are the collision and plasma wavelengths of the metal respectively [24].

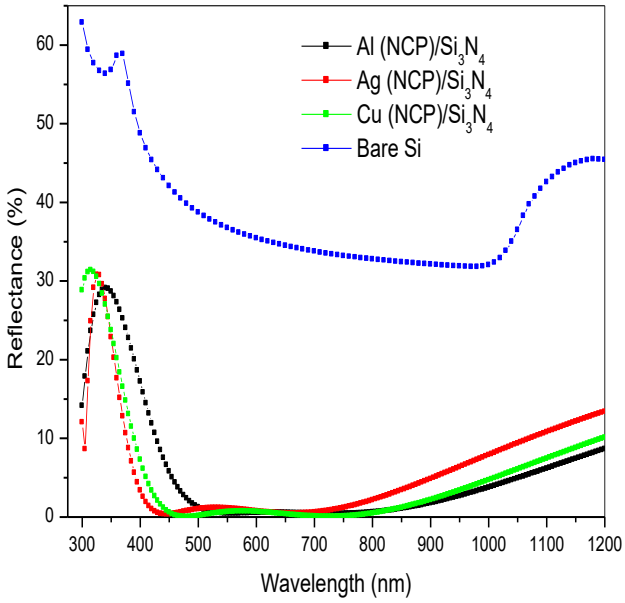

Fig. 2. The reflectance as a function of wavelength of incident radiation for bare silicon surface and Al, Ag, and Cu-NPs layer in combination of Si_3N_4 and silicon surface.

3. Results and Discussion

Fig. 2 displays the characteristic reflectance curves for silicon solar cells with and without ARCs. The plot illustrates that bare silicon exhibits reflectance above 30% across the entire spectral range, whereas with DLARC (NPs/Si_3N_4), reflectance appreciably decreases and nearly reaches zero over a wide spectral range. Reflectances are computed for nanoparticles of Cu, Al, and Ag over Si_3N_4. Notably, the reflectance for Cu nanoparticles is nearly zero in the spectral range of 450 – 800 nm.

In Fig. 3, the reflection is depicted as a function of the wavelength of incident radiation for Cu-nanoparticles with radii r = 20 nm, 40 nm, 48.5 nm, 60 nm, and 80 nm, spaced at intervals of 53 nm. The silicon nitride film thickness (region 3) is maintained at 60 nm. The plot reveals that reflection initially decreases with an increase in radius and then ascends. The minimum reflection is attained for nanoparticles with a radius of 48.5 nm.

Fig. 4 illustrates the reflectance plotted against various values of volume fractions of copper (f = 0.524, 0.430, 0.331, 0.219, 0.127, 0.081). It is evident from the figure that the minimum reflectance occurs at f = 0.219. Beyond this value, the reflectance is notably high, particularly at lower wavelengths (300 – 450 nm). Conversely, below f = 0.219, the influence of nanoparticles is nearly negligible, and the ARC structure behaves similar to a SLARC.

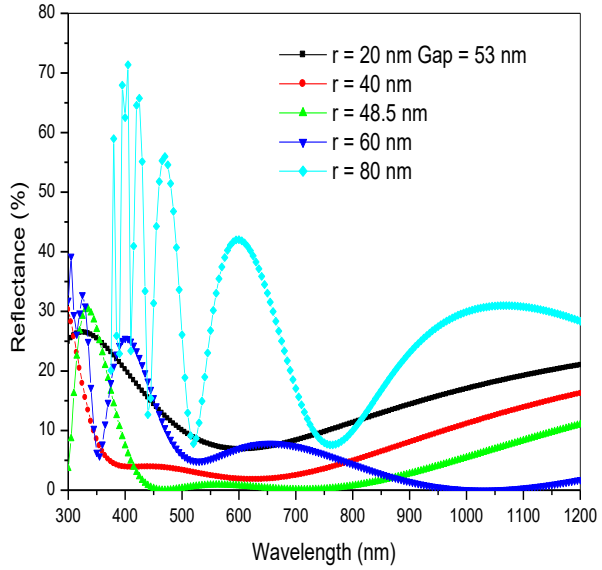

Fig. 3. Plot shows variation of reflectance as a function of wavelength of incident radiation for different radii of Cu-NPs.

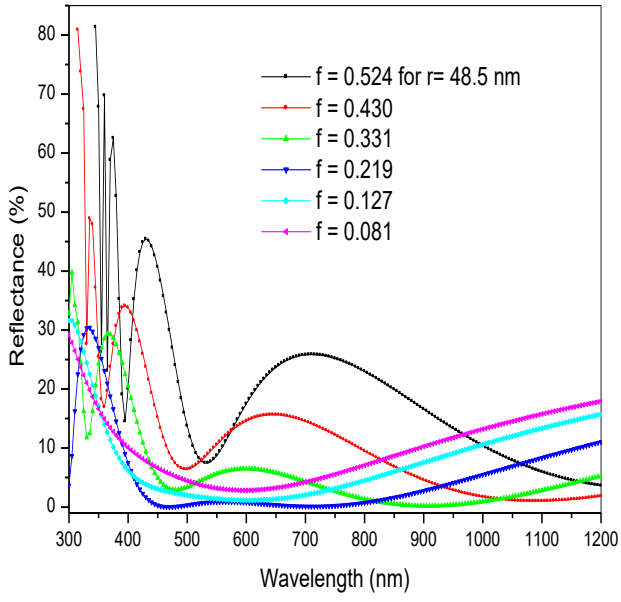

Fig. 4. Plot shows variation of reflectance as a function of wavelength of incident radiation for different value of volume fraction of Cu.

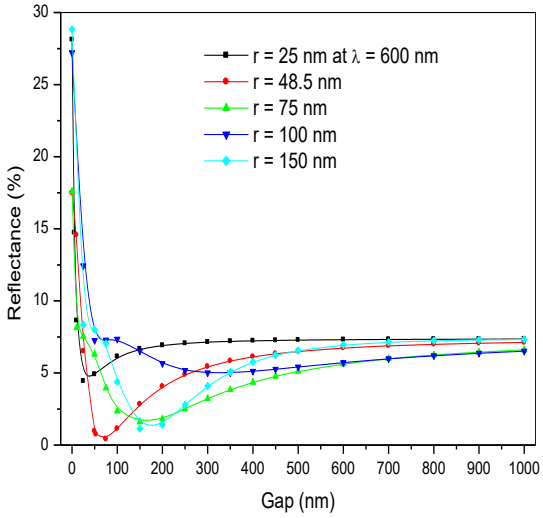

Fig. 5. Variation of reflectance as a function of gap size of nanoparticles of different radii.

The variation in reflectance as a function of the gap size of nanoparticles is also examined. In Fig. 5, reflectance is plotted against nanoparticles gap size for a wavelength of 600 nm and particle sizes of r = 25 nm, 48.5 nm, 75 nm, 100 nm, and 150 nm. The plot reveals that reflectance reaches a minimum between gap sizes of 53 nm and 200 nm. Beyond 200 nm, reflectance increases and stabilizes for nanoparticles of all sizes. Conversely, for gap sizes below 53 nm, reflectance steadily rises and reaches approximately 28 % for a zero gap size.

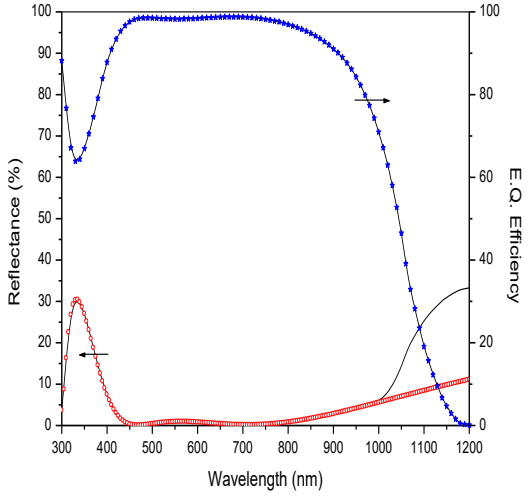

Fig. 6. Plot shows variation of reflectance and external quantum efficiency as a function of wavelength of incident radiations.

Table 1. Photovoltaic data of silicon solar cells with and without ARCs under AM 1.5 irradiation. (PC1D).

ARC Layer	I_{sc} (mA)	V_{oc} (V)	FF	η (%)
Without ARC	2.58	0.652	0.78	13.12
Si_3N_4	3.73	0.662	0.79	19.60
Cu-NPs/Si_3N_4	3.98	0.653	0.84	21.81

Further, the reflectance calculated for structure air/Cu-NPs/Si_3N_4/Si by TMM is used in PC1D simulator to study the performance of silicon solar cells. The specifications of copper nanoparticles are: radius = 48.5 nm, gap = 53 nm and volume fraction = 0.219 whereas device specifications (PC1D Simulator) are: material = Si, area = 100 cm^2, thickness = 200 µm, background doping (p-type) = 1×10^{16} cm^{-3}, front diffusion (n-type) = 1×10^{20} cm^{-3} and rear diffusion (p-type) = 1×10^{19} cm^{-3}. Fig. 6 shows a good agreement between the numerically calculated reflectance (symbols) and obtained from PC1D (solid line). External Quantum Efficiency (EQE) is a key parameter in solar cell performance, relating electrical outputs such as short-circuits current and conversion efficiency with optical properties like reflectance. Therefore, the performance of a solar cell can be effectively evaluated using both EQE and reflectance. Notably, when reflectance is minimized, EQE reaches its maximum, indicating improved light absorption and carrier generation. Figure 6 shows the variation of EQE as a function of wavelength of incident radiations. From figure one can observe that in the spectral range 450 – 800 nm the reflectance is nearly zero and EQE is 100 %. Finally, the solar cell parameters such as short circuit current (I_{sc}), open circuit voltage (V_{oc}), fill factor (FF) and photovoltaic efficiency (η) obtained from PC1D for the cell structure under consideration are 3.983 mA, 0.6533 V, 0.8382 and 21.81 % respectively. Photovoltaic data of silicon solar cells with and without ARCs under AM 1.5 irradiation is presented in the Table 1.

4. Conclusion

This study demonstrates the considerable improvement in the performance of silicon solar cells through the application of a double-layer anti-reflection coating composed of Cu-NPs and silicon nitride. By effectively reducing reflectance and enhancing light absorption, the Cu-NPs/Si_3N_4 ARC significantly boosts the external quantum efficiency, particularly in the spectral range of 450-800 nm. The optimized parameters of Cu-NPs: radius = 48.5 nm, gap size = 53 nm, and volume fraction = 0.219-yielded photovoltaic efficiency of 21.81 %. These findings emphasize the effectiveness of incorporating Cu-NPs in anti-reflection coatings to enhance the conversion efficiency of silicon solar cells.

References

1. R. Singh, J. Nanophotonics **3**, ID 032503 (2009). https://doi.org/10.1117/1.3196882
2. M. M. Shabat, S. A. Nassar, and H. G. Roskos; Romanian J. Phys. **65**, 609 (2020).
3. K. Ali, A. Sohail, and M. Z. M. Jafri, Int. J. Electrochem. Sci. **9**, 7865 (2014). https://doi.org/10.1016/S1452-3981(23)11011-X

4. K. C. Sahoo, M. Lin, E. Chang, Y. Lu, C. Chen, J. Huang, and C. Chang, Nanoscale Res. Lett. **4**, 680 (2009). https://doi.org/10.1007/s11671-009-9297-7
5. M. Moradi and Z. Rajabi, J. Nanostruc. **3**, 365 (2013).
6. R. Sharma, A. Gupta, and A. Virdi, J. Nano-Electron. Phys. **9**, ID 02001 (2012). https://doi.org/10.21272/jnep.9(2).02001
7. J. A. Dobrowolski, D. Poitras, P. Ma, H. Vakil, and M. Acree, Appl. Optics **41**, 3075 (2002). https://doi.org/10.1364/AO.41.003075
8. G. Hashmi, M. J. Rashid, Z. H. Mahmood, M. Hoq, and M. H. Rahman, J. Theoretical Appl. Phys. **12**, 327 (2018). https://doi.org/10.1007/s40094-018-0313-0
9. S. Lien, D. Wun, W. Yeh, and J. Liu, Sol. Energ. Mat. Sol. Cells **90**, 2710 (2006). https://doi.org/10.1016/j.solmat.2006.04.001
10. A. Bahrami, S. Mohammadnejad, N. J. Abkenar, and S. Soleimaninezhad, Int. J. Renew. Energ. Res. **3**, 79 (2013).
11. M. Medhat, S. EL-Zaiat, S. Farag, and G. Youssef, Turkish J. Phys. **40**, 30 (2016). https://doi.org/10.3906/fiz-1508-14
12. R. Sharma, Turkish J. Phys. **42**, 350 (2018). https://doi.org/10.3906/fiz-1801-28
13. S. Pillai, K. R. Catchpole, T. Trupke, and M. A. Green, J. Appl. Phys. **101**, ID 093105 (2007). https://doi.org/10.1063/1.2734885
14. H. C. Lee, S. C. Wu, T. C. Yang, and T. J. Yen, Energies **3**, 784 (2010). https://doi.org/10.3390/en3040784
15. D. M. Schaadt, B. Feng, and E. T. Yu, Appl. Phys. Lett. **86**, ID 063106 (2005). https://doi.org/10.1063/1.1855423
16. D. Qu, F. Liu, J. Yu, W. Xie, Q. Xu, X. Li, and Y. Huang, Appl. Phys. Lett. **98**, ID 113119 (2011). https://doi.org/10.1063/1.3559225
17. E. C. Wang, S. Mokkapati, T. Soderstrom, S. Varlamov, and K. R. Catchpole, IEEE J. Photovolt. **3**, 267 (2013). https://doi.org/10.1109/JPHOTOV.2012.2210195
18. T. L. Temple, G. D. K. Mahanama, H. S. Reehal, and D. M. Bagnall, Sol. Energy Mater. Sol. Cell **93**, 1978 (2009). https://doi.org/10.1016/j.solmat.2009.07.014
19. H. A. Atwater and A. Polman, Nature Mater. **9**, 205 (2010). https://doi.org/10.1038/nmat2629
20. M. F. Ubeid, M. M. Shabat, and J. Charrier, Romanian Rep. Phys. **72**, 415 (2020).
21. S. A. Abuibaid, H. M. Mousa, M. M. Shabat, and D. M. Schaadt, Romanian J. Phys. **66**, 602 (2021).
22. R. Sharma, Heliyon **5**, ID e01965 (2019). https://doi.org/10.1016/j.heliyon.2019.e01965
23. H. A. Macleod, Thin Film Optical Filters, 2nd Edition, London Institute of Physics (Tailor and Francis Group, 2001). https://doi.org/10.1201/9781420033236
24. N. K. Sharma, Indian Acd. Sci. **78**, 417 (2012). https://doi.org/10.4103/0378-6323.98071
25. S. R. Mirnaziry, M. A. Shameli, and L. Yousefi, Sci. Rep. **12**, 13259 (2022). https://doi.org/10.1038/s41598-022-17677-z